

Phase Information and the Evolution of Cosmological Density Perturbations

Lung-Yih Chiang¹ and Peter Coles^{1,2}

¹ *Astronomy Unit, School of Mathematical Sciences, Queen Mary & Westfield College, London E1 4NS, UK.*

² *School of Physics & Astronomy, University of Nottingham, University Park, Nottingham NG7 2RD, UK.*

5 August 2021

ABSTRACT

The Fourier transform of cosmological density perturbations can be represented in terms of amplitudes and phases for each Fourier mode. We investigate the phase evolution of these modes using a mixture of analytical and numerical techniques. Using a toy model of one-dimensional perturbations evolving under the Zel'dovich approximation as an initial motivation, we develop a statistic that quantifies the information content of the distribution of phases. Using numerical simulations beginning with more realistic Gaussian random-phase initial conditions, we show that the information content of the phases grows from zero in the initial conditions, first slowly and then rapidly when structures become non-linear. This growth of phase information can be expressed in terms of an effective entropy: Gaussian initial conditions are a maximum entropy realisation of the initial power-spectrum, gravitational evolution *decreases* the phase entropy. We show that our definition of phase entropy results in a statistic that explicitly quantifies the information stored in the phases of density perturbations (rather than their amplitudes) and that this statistic displays interesting scaling behaviour for self-similar initial conditions.

Key words: cosmology: theory – large-scale structure of the Universe – methods: statistical

1 INTRODUCTION

Observations of large-scale structure in the spatial distribution of galaxies pose some of the most interesting challenges facing modern cosmological theory. Prominent among the issues raised by the confrontation is the question of how to best to use the information contained in maps of galaxy positions to constrain theoretical models.

Traditional methods for the analysis of such maps involves a Fourier decomposition, treating the cosmological density contrast as a superposition of plane waves with (complex) amplitudes $\tilde{\delta}_k$:

$$\delta(\mathbf{x}) = \frac{\rho(\mathbf{x}) - \rho_0}{\rho_0} = \sum \tilde{\delta}_k \exp(i\mathbf{k} \cdot \mathbf{x}), \quad (1)$$

where ρ_0 is the mean matter density. We discuss this kind of spectral representation in more detail in Section 4. The statistical analysis of galaxy clustering generally proceeds via the properties of the amplitudes $\tilde{\delta}_k$. A particularly useful statistical quantity in this respect is the power spectrum, essentially proportional to $|\tilde{\delta}_k|^2$, which is a second-order statistic in Fourier space. Higher order quantities based on $\tilde{\delta}_k$ can also be found, such as the bispectrum (Peebles

Figure 1. A simple demonstration of the importance of phase information for pattern morphology. Panel (a) shows an example realisation of an N-body experiment with initial random phases. Panel (b) is obtained by taking the Fourier transform of panel (a), setting all the amplitudes to a constant ($|\tilde{\delta}_k| = 1$) then taking the inverse Fourier transform; it therefore retains only the phase information from (a). In panel (c), each mode keeps the same amplitude so the power-spectrum is unchanged but we redistribute the phases randomly among the modes. It is easy to see the striking resemblance between (a) and (b), the phase-only reconstruction, but (c) which has the same power-spectrum but random phases, is featureless.

1980; Matarrese, Verde & Heavens 1997) or through correlations of $\tilde{\delta}_k^2$ (e.g. Stirling & Peacock 1996). However, an alternative approach exists that has not been explored greatly in the cosmological literature, and that is to look explicitly not at the amplitudes (the moduli of $\tilde{\delta}_k$) but their *phases* ϕ_k where

$$\tilde{\delta}_k = |\tilde{\delta}_k| \exp(i\phi_k). \quad (2)$$

The importance of phase information can be understood by considering a simple example. Gaussian white noise consists of a superposition of Fourier modes with random phases and whose amplitudes are drawn from a distribution which is independent of wavenumber, i.e. a flat spectrum. Now imagine a density field represented as a single Dirac δ -function in a periodic volume. The Fourier transform of this density field is constant in amplitude, so that its power spectrum corresponds exactly to the white noise spectrum. What differs drastically in these two cases is the difference in phases. In the former, the phases are random, in the latter, the phase of each mode is a definite relationship to the other modes resulting in a real-space distribution that is strongly localised. This second distribution clearly represents a more *ordered* state than the first one, but their power spectra are identical. A more relevant example is shown in Figure 1. The left panel shows a grey-scale representation of the density field obtained from a two-dimensional N-body simulation. In the centre panel, the amplitudes of the Fourier components are set to a constant value, but the phases are retained. The morphology of the density field is very similar to the original. The result of randomly reshuffling the phases but retaining the amplitudes is shown on the right; information about the shape of the original pattern is destroyed. One can conclude from these examples that key information about the shape of localised features in a spatial pattern resides in the distribution of phases, and that information should in principle be quantifiable. Further interesting general examples of the importance of phase information for the analysis of images (in the widest sense of the word) can be found in Oppenheim & Lim (1981). The question is, how to quantify the information content of the distribution of phases?

The density distributions of interest in cosmology are, of course, more complicated than these toy examples. Moreover, since gravitational clustering is generally thought to be driven by the process of gravitational instability we need to understand not only the phase information in “snapshots” of the density field, but the way in which phase information evolves with time.

The standard model for the formation of galaxies and large-scale structure involves the idea that these structures grew by the action of gravitational instability from small initial density perturbations present in the early Universe. In most popular variants of this model, particularly those involving cosmic inflation, the initial perturbations are Gaussian, meaning amongst other things that their probabilistic properties are completely specified by knowledge of second-order statistical quantity: the autocovariance function, or its Fourier transform the power spectrum discussed above. Gaussian random fields are useful not only because of this very economical prescription of their statistical properties, but also because many properties of Gaussian random density fields can be calculated analytically (e.g. Bardeen et al. 1986). One particularly interesting property of Gaussian random fields is that they possess Fourier modes whose real and imaginary parts are independently distributed or, in other words, that they have phases which are independently distributed and uniformly random on the interval $[0, 2\pi]$. Terms in the evolution equations for the Fourier modes that represent coupling between different modes are of second (or higher) order in δ and these are neglected when first-order perturbation theory is considered. During the linear regime, therefore, Fourier modes evolve independently and the phases remain independent and uniformly random (Peebles 1980; Sahni & Coles 1995). In the later stages of evolution, however, modes begin to couple together. It is in this regime that information flows into the set of Fourier phases.

There are therefore two reasons for studying phase correlations. One is to understand exactly how the morphology of non-linear clustering pattern is driven by the growth of phase information. The other is to explore ways of testing the initial hypothesis of Gaussian initial conditions, using measurements of phase association to constrain the level of possible non-Gaussianity.

Some papers on this subject refer to the appearance of phase information in terms of *phase correlations*. In a strict sense of the word correlation, which means association expressed through second-order quantities such as covariances, this is incorrect. As we show in Section 4, any statistically homogeneous field cannot display phase correlations. However, it is certainly true that phases are no longer independently distributed in this regime.

Despite the clear importance of phases for the morphology of galaxy clustering, the relevant literature is relatively sparse, with most attention being focused on the evolution of individual phases away from their initial values (Ryden & Gramman 1991; Soda & Suto 1992; Jain & Bertschinger 1998). One notable exception is the work by Scherrer, Melott & Shandarin (1991) who suggested and explored a method of quantifying phase association that could be applied to real data. The sparsity of the existing literature on phases is at least partly due to the difficulty in developing statistical methods for quantifying phase information, a difficulty we attempt to address in this work.

In this paper we discuss the phase evolution and the quantification of the information they represent. After presenting some relevant background in Section 2, we begin by exploring the evolution of phases using simplified 1D

analytical models in Section 3. This study suggests a simple way of encoding phase information which we present in Section 5. With the aid of dynamical numerical simulations in Section 6, we present how the encoded information from phases evolves with different initial conditions and displays interesting behaviour for self-similar evolutions. In Section 7, we discuss the results and offer suggestions on how phase information might be extracted from real surveys.

2 THEORETICAL BACKGROUND

2.1 Linear Perturbation Theory

For the purposes of this study we consider a spatially flat matter-dominated universe. If the mean free path of the particles is small, it is appropriate to treat the large-scale distribution of matter as a self-gravitating Newtonian fluid with zero pressure. In this case the evolution of the gravitating system can be described in a comoving frame by the following three equations: the *continuity equation*,

$$\frac{\partial \delta}{\partial t} + \frac{1}{a} \nabla_{\mathbf{x}}[(1 + \delta)\mathbf{v} = 0; \quad (3)$$

Euler equation,

$$\frac{\partial(a\mathbf{v})}{\partial t} + (\mathbf{v} \cdot \nabla_{\mathbf{x}})\mathbf{v} = -\frac{1}{\rho} \nabla_{\mathbf{x}}p - \nabla_{\mathbf{x}}\phi; \quad (4)$$

and Poisson equation,

$$\nabla_{\mathbf{x}}^2\phi = 4\pi G a^2 \rho_0 \delta. \quad (5)$$

In these equations $\delta(\mathbf{x})$ is the density contrast defined by eq. (1); for a spatially flat and matter-dominated universe the mean density $\rho_0 = 1/6\pi G t^2$. In the equations (3-5), $\nabla_{\mathbf{x}}$ denotes a derivative with respect to the comoving coordinates \mathbf{x} , where $\mathbf{x} = \mathbf{r}/a(t)$, and \mathbf{r} are proper coordinates. The velocity field is $\mathbf{v}(\mathbf{x}, t) = a\dot{\mathbf{x}}$ and $\phi(\mathbf{x}, t)$ is the peculiar gravitational potential. The regime in which $\delta \ll 1$, permits one to linearise (3) and (4) by keeping only terms of first order in the perturbed quantities. We thus obtain

$$\frac{\partial^2 \delta}{\partial t^2} + 2\left(\frac{\dot{a}}{a}\right) \frac{\partial \delta}{\partial t} - 4\pi G \rho_0 \delta = 0. \quad (6)$$

Solving this equation with the initial condition $\delta(\mathbf{x}, t_i) = \delta_0(\mathbf{x})$ and $\dot{\delta}(\mathbf{x}, t_i) = 0$ at t_i , when the perturbations start growing, we get

$$\delta(\mathbf{x}, t) = \delta_0 b_{\pm}(t), \quad (7)$$

with the growing mode, $b_+ \propto t^{2/3}$, and the decaying mode, $b_- \propto t^{-1}$. This solution describes the growth of perturbations at early times. In this regime the evolution of each individual Fourier mode, $\tilde{\delta}_k$, of δ is decoupled from the other modes and its rate of growth is independent of k .

The linear solution breaks down when δ is compatible with unity or beyond, because terms of higher order than the linear terms become important. To probe the onset of non-linearity we therefore need to use more sophisticated approximation methods than first-order perturbation theory (see, e.g. Sahni & Coles 1995, for a thorough review).

2.2 The Zel'dovich Approximation

Zel'dovich (1970) proposed a particularly ingenious approximate scheme which can be used to extrapolate the evolution of density fluctuations well into the non-linear regime. In the eponymous Zel'dovich approximation (ZA), a particle initially placed at Lagrangian coordinate \mathbf{q} finds itself after a time t at an Eulerian coordinate \mathbf{x} . The displacement it has experienced simply depends on the velocity the particle had when it was at its original position, through $b(t)\mathbf{u}(\mathbf{q})$, so that

$$\mathbf{r}(\mathbf{q}, t) = a(t)\mathbf{x}(\mathbf{q}, t) = a(t)[\mathbf{q} + b(t)\mathbf{u}(\mathbf{q})], \quad (8)$$

where $a(t)$ is the expansion factor and $b(t)$ is the growing mode b_+ in (7). According to this prescription, the motion of the medium is simply Newtonian inertial motion: each particle moves with its original velocity along a ballistic trajectory. [Note that the peculiar velocity according to the Zel'dovich approximation is $a\dot{\mathbf{x}} = a(t)\dot{b}(t)\mathbf{u}(\mathbf{q})$.] For an irrotational flow, $\mathbf{u}(\mathbf{q})$ can be expressed as a gradient of some velocity potential $-\nabla\Phi_0(\mathbf{q})$.

The evolutionary picture that the Zel'dovich approximation suggests is that particles set out on inertial trajectories with their initial velocities determined by the initial velocity potential $\Phi_0(\mathbf{q})$ and follow straight lines with constant velocities. When two such trajectories meet, a singularity forms and both their positions, being distinct in

Lagrangian space, are mapped onto the same Eulerian coordinate. Such a singularity is called a *caustic* and its formation is called *shell-crossing*. Because the Zel'dovich approximation does not deal properly (or, indeed, at all) with the self-gravity of regions formed when such caustics occur, the two particles entering the singularity do not coalesce in a bound structure, but their paths cross each other and form multi-stream flows. The approximation breaks down at this point, and the mapping from Lagrangian to Eulerian space can no longer be inverted. Nevertheless, before shell crossing, the Zel'dovich approximation provides an excellent approximation to the real evolution of the density contrast (e.g. Coles, Melott & Shandarin 1993).

Before shell-crossing the evolution of δ can be determined which can be obtained by requiring mass conservation between Lagrangian and Eulerian space

$$\rho_0 d^3 q = \rho(\mathbf{x}, t) d^3 x. \quad (9)$$

If the flow is assumed irrotational, the matrix $\partial x_i / \partial q_j$ is a symmetric matrix and can be diagonalised. Therefore,

$$\rho(\mathbf{x}, t) = \frac{\rho_0}{(1 - b(t)\lambda_1)(1 - b(t)\lambda_2)(1 - b(t)\lambda_3)}, \quad (10)$$

if $-\lambda_1, -\lambda_2, -\lambda_3$ are the eigenvalues of $\partial u_i(q) / \partial q_j$. Thus, the condition that a caustic forms is the same condition as that one eigenvalues of the matrix $\partial x_i / \partial q_j$ should be equal to $1/b(t)$.

The Zel'dovich approximation breaks down entirely in the highly non-linear regime, but this is not too great a problem for the problem at hand. As other studies of phase evolution have shown (Ryden & Gramman 1991; Scherrer, Melott & Shandarin 1991; Soda & Suto 1992; Jain & Bertschinger 1998), the phases of Fourier modes ϕ_k begin to move very rapidly away from their original values ϕ_i when density fluctuations become very large. This poses a problem for the interpretation of phase information when each one wraps around many multiples of 2π . In fact, what happens in the non-linear regime is that phases move so quickly for short-wavelength modes that their displacements become very much larger than 2π . The ‘observed’ phases, measured modulo 2π , then appear random because of the heavy phase wrapping in the strongly non-linear regime. This is a difficult problem to deal with, so we will simply skirt around it and consider only what happens on scales just entering the non-linear regime.

2.3 The Zel'dovich Approximation in One Dimension

Although the Zel'dovich approximation (ZA) is a very useful tool for following the fully three-dimensional evolution of density perturbations, it is particularly noteworthy that the solution it provides in one dimension is exact, at least until the first shell-crossing. In one dimension, including the case of a single plane wave in 3D, the value of δ calculated from the Poisson equation is the same as that found using the ZA. The ZA is therefore a particularly useful tool to explore the evolution of the density contrast in 1D; every particle carries information about its position and velocity during the evolution. In one dimension, the ZA is simply

$$x(q, t) = q - b(t) \frac{d\Phi_0(q)}{dq}, \quad (11)$$

and the density contrast is

$$\delta = \left(\frac{\partial x}{\partial q} \right)^{-1} - 1 = \left(1 - b(t) \frac{d^2\Phi_0(q)}{dq^2} \right)^{-1} - 1, \quad (12)$$

until the first singularity develops, at which point

$$\frac{dx}{dq} = 0, \quad (13)$$

or

$$b(t) = \left(\frac{d^2\Phi_0(q)}{dq^2} \right)_{\min}^{-1}. \quad (14)$$

The velocity potential field is closely related to gravitational potential field, but it is important to realise that this is only relevant to the initial velocities of particles and not to their final positions; density peaks take place, not at the minima of potential wells, at the positions where the change of curvature in the potential field is zero, i.e. $d^3\Phi_0/dq^3 = 0$ with $d^4\Phi_0/dq^4$ at their minima.

The fact that the ZA is exact in one dimension until shell-crossing allows us to study this case with particular ease (cf. Soda & Suto 1992). What we shall do in the next section is to study the evolution of phases in 1D in order to gain at least a qualitative understanding of how non-linear evolution leads to an increase in the information content of the set of Fourier phases. These calculations represent, for the time being, toy models, but as we shall see they will lead to the suggestion of a very useful way of quantifying phase evolution in the more general case.

3 ONE-DIMENSIONAL ANALYTIC CALCULATIONS

The Fourier transform of the density contrast $\delta(x)$ in one dimension can be expressed as

$$\tilde{\delta}_k = \frac{1}{2\pi} \int_{-\pi}^{\pi} \delta(x) \exp(ikx) dx = \Delta_k e^{i\phi_k}, \quad (15)$$

where ϕ_k is the phase of the k -th mode, and $\Delta_k = |\tilde{\delta}_k|$, which is real, is its amplitude; c.f. equation (2). Here it is assumed that the universe is periodic in one dimension with a period of 2π , i.e. $x(q + 2j\pi) = x(q)$. Typically, we can represent the velocity potential as the sum of sinusoidal functions, i.e.

$$\Phi_0(q) = \sum_k A_k \cos(kq + \alpha_k); \quad (16)$$

the assumption of periodicity requires that k here must be an integer.

Getting an analytic solution for the Fourier modes of the density distribution evolved according to the Zel'dovich approximation is not as straightforward as one might think because the Fourier transform (15) is made from real-space Eulerian coordinate, which in turn represents a mapping from the Lagrangian coordinate. From (15)

$$\delta_k = \frac{1}{2\pi} \int_{-\pi}^{\pi} \left[\left(\frac{dx}{dq} \right)^{-1} - 1 \right] e^{ikx} dx = \frac{1}{2\pi} \int_{-\pi}^{\pi} e^{ikx} dq = \frac{1}{2\pi} \int_{-\pi}^{\pi} \exp \left[ik \left(q - b(t) \frac{d\Phi_0(q)}{dq} \right) \right] dq. \quad (17)$$

Obviously, the case of an arbitrary $\delta(x)$ comprising a number of different Fourier modes is going to be difficult to analyse, so we will begin by looking at simpler cases.

3.1 Single Mode

The simplest case we can consider is one in which the velocity potential is described by a velocity potential comprising a single sinusoidal function:

$$\Phi_0(q) = -\cos(q + \alpha). \quad (18)$$

An analytical solution is available in this case

$$\tilde{\delta}_k = \frac{1}{2\pi} \int_{-\pi}^{\pi} dq \exp\{ik[q - b(t) \sin(q + \alpha)]\} = \exp(-ik\alpha) J_k[kb(t)], \quad (19)$$

where $J_k[kb(t)]$ is the *Bessel* function of the k -th order and the phase $\phi_k = -k\alpha$ (Shandarin & Zel'dovich 1989). When $b(t) \ll 1$, $\Delta_k \propto [kb(t)]^k$, indicating the amplitudes of low-frequency modes grow faster than those of high-frequency ones. As $b(t)$ is approaching unity, the time when the first caustic forms, the amplitude for $k = 1$ slows down, compared with the extrapolation of the linear theory (in which the amplitudes grow with the same rate). The phases, on the other hand, remain the same until shell-crossing. This idealised case demonstrates that the collapse of a single plane wave involves the generation of higher-frequency modes with phases determined by the phase of the original mode.

3.2 Double Mode

The next case we consider is where the initial velocity potential is simply the superposition of two sinusoidal forms:

$$\Phi_0(q) = -\cos(k_1 q) - \cos(k_2 q + \alpha). \quad (20)$$

Even in this very simple case, no analytical solution can be obtained. We begin with a particular choice of frequencies for the two starting modes, one being the fundamental mode $k_1 = 1$ and the other being double this frequency. In Figure 2, we show five different values of α for $k_1 = 1$ and $k_2 = 2$: $\alpha = 0.3, 1.1, 2.0, 2.8$, and 3.1 . The first row shows the corresponding velocity potential. There are two wells in the potential field; consequently two density peaks form during the later stages of evolution, shown in the second row. The density contrast δ is plotted against q when $b(t) = 0.2$ for all five α 's. The choice of this $b(t)$ value is arbitrary but to show density contrast at very late stage from which phase coupling in Fourier domain can be explored. According to equation (14), different velocity potential fields have different times for the first shell-crossing, so δ in Figure 2 shows different levels of density peaks. In order to elucidate the pattern of phases generated by the evolution of this system, we use a technique borrowed from the idea of a *return map* used in chaotic dynamics (e.g. May 1976).

To analyse a chaotic time series $X(t)$, sampled at discrete times t (which we assume to be represented by the integers), it is useful to plot X_{t+1} against X_t for each pair of consecutive values $(t, t+1)$; this is the return map.

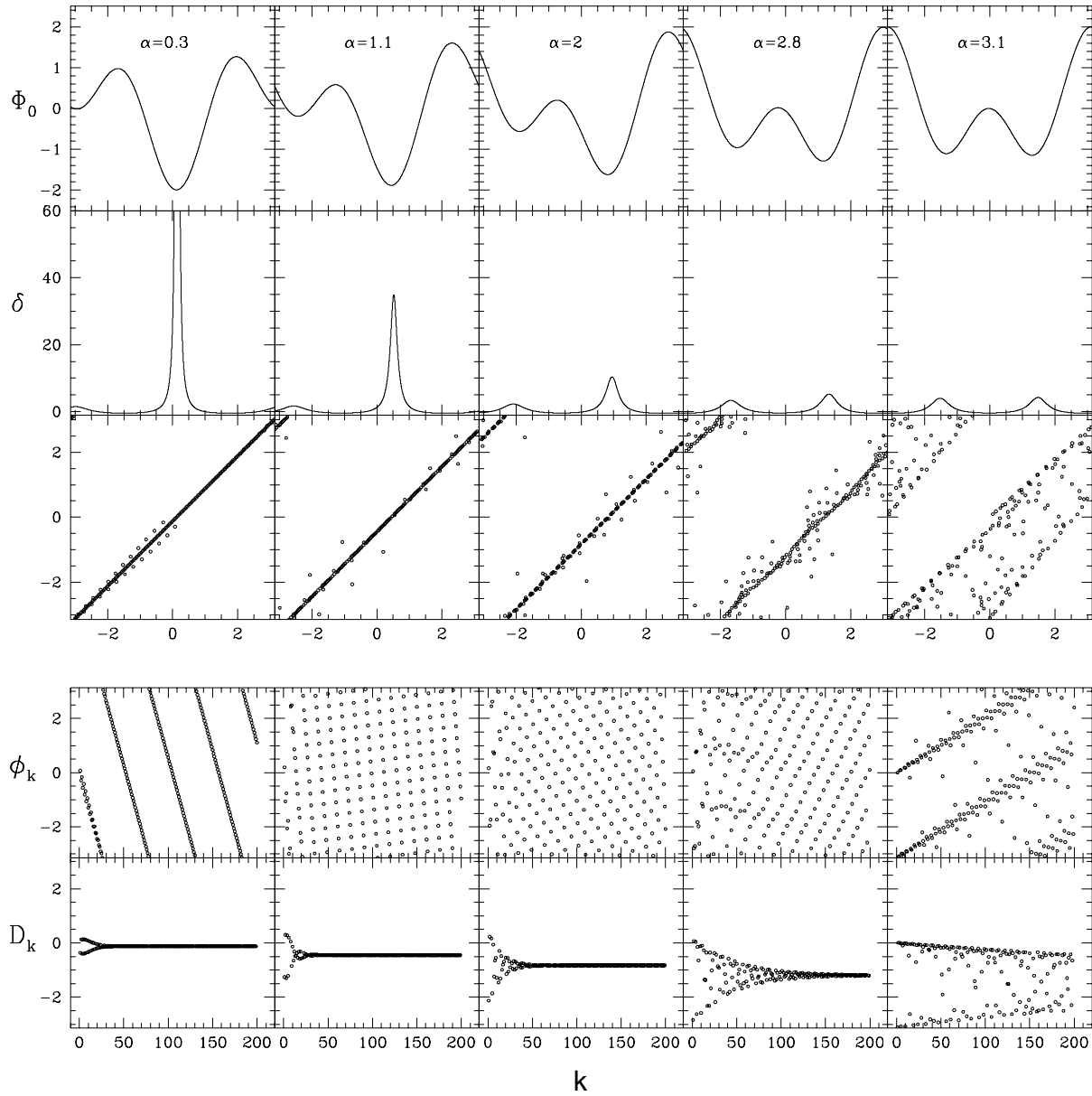


Figure 2. Double-mode calculations with $(k_1, k_2) = (1, 2)$. Five different values of α are drawn for one-dimensional ZA solutions with an initial velocity potential $\Phi_0 = -\cos(q) - \cos(2q + \alpha)$. There are two potential wells in Φ_0 , causing two density peaks to form. The second row is the density contrast δ when $b(t) = 0.2$. Both Φ_0 and δ are periodic between $-\pi$ and π , and are shown as functions of the Lagrangian coordinate q . The third row is the corresponding return map, ϕ_{k+1} versus ϕ_k , both of which are measured modulo 2π . The fourth and fifth rows are the phase ϕ_k and discrete phase gradient D_k , respectively, both being drawn against k . Histograms of the phases ϕ_k show a uniform distribution, whereas in the return maps the coupling of consecutive phases is clear. The relationship between the formation of density contrast and the way phases couple each other is easy to see via D_k panels. A dominant density peak converges D_k on large k , whereas the shape of D_k on small k 's depends on the morphology of the structure. If two compatible density peaks form at the same time, D_k converges slowly towards large k 's.

If X_t and X_{t+1} are independent then the result should be a scatter plot in which no pattern appears. A time series consisting of correlated noise, would show some correlation in its return map, whereas a chaotic series would exhibit some form of attractor. We adapt this idea to the case in hand, by considering the sequence of phases ϕ_k in the same way. For a ϕ_k sequence of a density distribution, ϕ_k are paired for all modes as points (ϕ_k, ϕ_{k+1}) in a return map so that one can hope to see some pattern emerging in the relationship between two successive phases. This idea can, in principle, be generalised to higher-order maps showing ϕ_{k+2} against ϕ_k , etc.

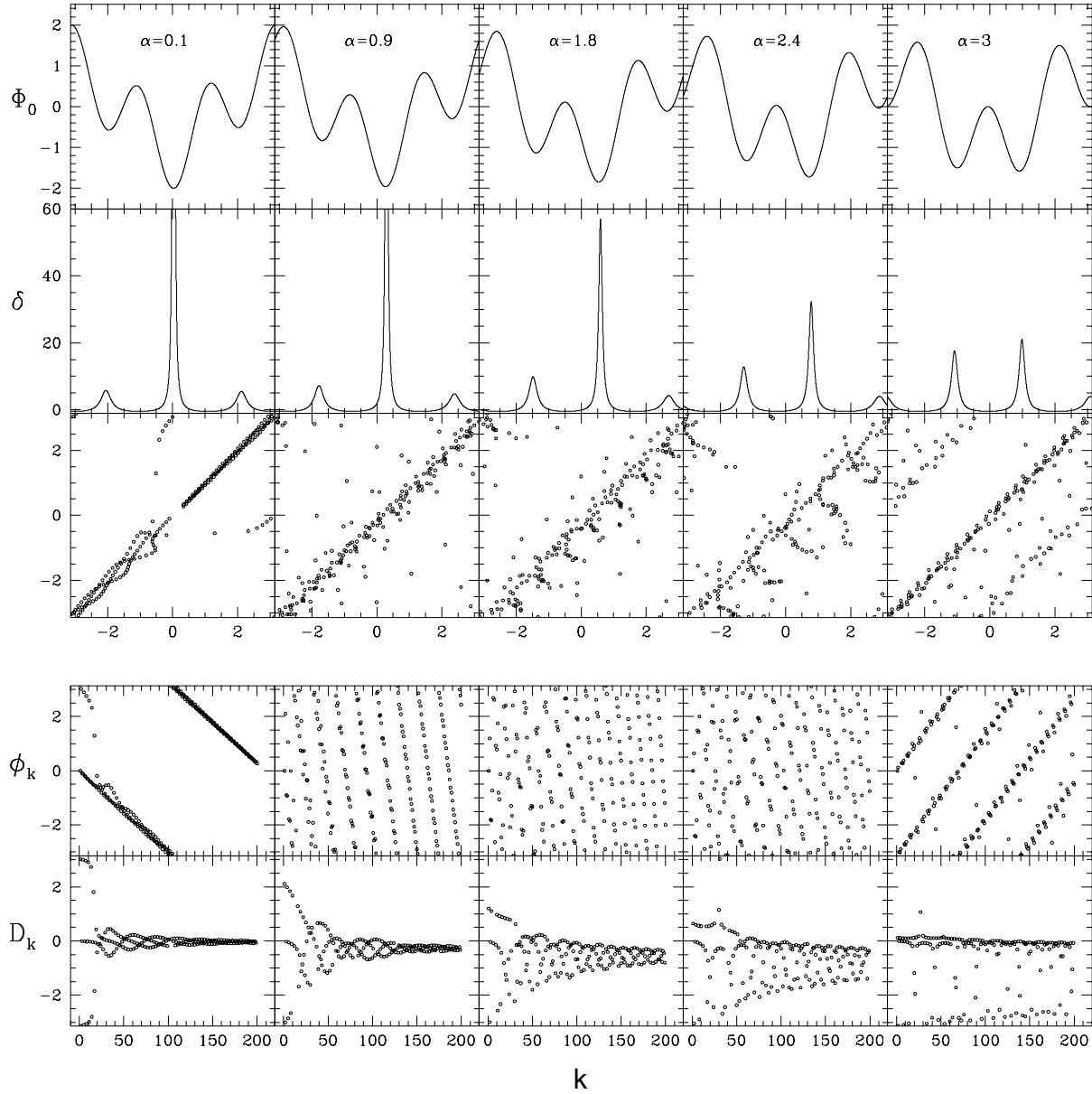


Figure 3. $(k_1, k_2) = (1, 3)$ for double mode. All the notations follow those in Figure 2. Here three potential wells cause three density peaks. δ is drawn when $b(t) = 0.1$. The return map is more complicated in this case, but D_k plots show the same relationship between consecutive phases as that in Figure 2. A dominant peak causes D_k to converge more quickly towards large k than two compatible ones.

For the case of the single mode, the ϕ_k sequence decreases monotonically by fixed quantity α for each step in k . In the return map, the phases are mapped into points $\{(\phi_1, \phi_2) = (-\alpha, -2\alpha), (\phi_2, \phi_3) = (-2\alpha, -3\alpha) \dots\}$, which forms in the return map a diagonal line, provided that α is not a rational multiple or fraction of π .

Before examining the possible patterns in the return maps, we show in the fourth row of Figure 2 the phase ϕ_k as a function of k . Even for the simplest case of two density peaks, the phases display a complicated behaviour among these five different values of α . In the return maps, however, it is clear to see the patterns for the corresponding density distributions. The diagonal lines in the first three panels are from the mapping of consecutive phases of high-frequency modes, which resemble the single-mode case. The points oscillating with the diagonal lines are from phases of long-wavelength modes. When α approaches π , the phases are mapped into regions, instead of one single line.

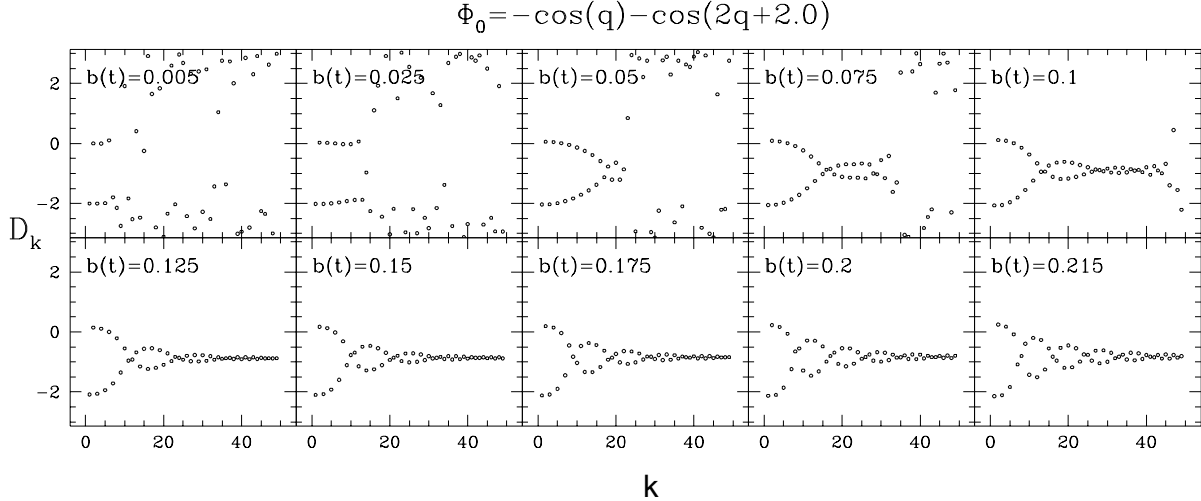


Figure 4. The evolution of discrete phase gradient for $\Phi_0 = -\cos(q) - \cos(2q + 2.0)$. The phase gradient D_k is shown as a function of k up to $k = 50$. In the top left panel, phases from small k 's start coupling at the beginning of the evolution, which depends on the initial phase difference between the two sinusoids, whereas those of high-frequency modes, whose amplitudes at this stage are still small or zero, are rounding errors. As the density fluctuation grows, fine details appear when higher harmonics are spawned by the collapsing waves with a definite phase relationship leading to sharp peaks that eventually become caustics.

A similar effect is noticed in Figure 3. Again, five different potentials with different values of α are drawn for $k_1 = 1$, and $k_2 = 3$. All the notations follow those in Figure 2. Three potential wells cause three density peaks when $b(t) = 0.1$. We see again in the ϕ_k panels phases seem randomly distributed as in Figure 2. In the return maps, phases are not mapped onto diagonal lines, but much more complicated patterns. As the patterns are the mapping from ϕ_k to ϕ_{k+1} , we devise a new quantity to look for how the consecutive phases are coupled

$$D_k = \phi_{k+1} - \phi_k, \quad (21)$$

which means that D_k is effectively a discrete phase gradient. As will become clear in the next few sections, a histogram from D_k can be used to quantify phase information. Plotting a histogram of the ϕ_k , however, is a useless diagnostic of phase correlations. Such a plot would involve the projection of the return map onto one or other of the axes. Even if ϕ_k and ϕ_{k+1} were linearly related, the histogram of phases would be uniform, as can be seen from Figure 2. Instead of taking D_k series into the return map, we plot the discrete phase gradient D_k against k in the fifth row both in Figure 2 and Figure 3. In Figure 2, the successive phases are coupled in such a way that the series of $D_k|_{k=1,3,5\dots}$ and $D_k|_{k=2,4,6\dots}$ twine together and oscillate embedded in a decay, and in Figure 3, it is $D_k|_{k=1,4,7\dots}$, $D_k|_{k=2,5,8\dots}$ and $D_k|_{k=3,6,9\dots}$ that shows a definite relationship between phases.

Since phases alone can recover the morphology of the structure, what is shown in D_k for $(k_1, k_2) = (1, 2)$ case can be demonstrated and understood qualitatively by two Gaussian waves, or three for $(k_1, k_2) = (1, 3)$, the reason being Gaussian function is easy to manipulate between real and Fourier domain. It turns out that the resulting $\tilde{\delta}_k$ of mode k is from vector superposition in the complex plane, i.e., $\tilde{\delta}_k^{(1)} + \tilde{\delta}_k^{(2)}$, both being the k -th mode of Fourier transform of two density peaks. The number of twining series was caused by the number of density peaks. When $\alpha = \pi$, two identical peaks located at q_1 and $-q_1$ form symmetrically to the origin in real domain, so phases of the k -th mode is formed by superposition in the complex plane of two vectors with same amplitude, whose phases are kq_1 and $-kq_1$, multiples of the fundamental mode and always symmetric to the x -axis. This results in $\phi_k = 0$ or π , so D_k flip between 0 and π . Bearing this picture in mind, we can understand qualitatively why, when α is small, the dominant sharp peak produces fast convergence of D_k on high-frequency modes, similar to the single-mode solution, whereas the twining part of D_k depends on the morphology of the distribution. The vector in the complex plane representing the dominant sharp peak has much larger amplitude than the other one. This fast convergence of D_k results from receding influence of vector superposition on the resulting ϕ_k from the vector which represents the less dominant density wave. Moreover, when α is tuned approaching π , a dominant sharp peak is replaced by two compatible ones, whose locations are shifting towards symmetry to the origin in real domain, so two compatible vectors in the complex plane account for the slow convergence in D_k . Therefore, the degree of convergence in D_k depends on how asymmetrical are the representational vectors for the sinusoids are in the complex plane.

Figure 4 shows the evolution of the discrete phase gradient for the case of $\Phi_0 = -\cos(q) - \cos(2q + 2.0)$. At the initial condition, only two modes have well-defined amplitudes and so only two phases really exist. However, rounding errors in the evaluation of the required integrals result in the assignment of a definite phase even to those modes which have formally zero amplitude. These fictional phases are initially random when the evolution begins. The first structure appeared in D_k depends on the phase difference between the two sinusoids, in which D_k from low-frequency modes flip between 0 and $-\alpha$. Fine details of the structure appear when higher harmonics are spawned by the collapsing waves with a definite phase relationship leading to sharp peaks that eventually become caustics. Those spawned modes not only produce the twining characteristic in D_k , but also interfere with the phases of low-frequency modes.

3.3 Comments

We have analysed these simple cases of two interacting plane waves in an attempt to develop a quantitative understanding of the kind of structure one can hope to see in the phases of non-linearly evolved density fields.

The results obtained depend very sensitively on the initial phase difference. The reason for this is that different real-space processes become confused when viewed in the Fourier domain, particularly in the phase representation. For one thing, each initial sinusoid begins to collapse in the same manner as the single-mode solution described in §3.1. This spawns Fourier modes with a definite phase relationship to the initial mode. This process generates high-frequency modes which interfere and produce a pattern in the return map that depends quite sensitively on the symmetry of the situation, i.e. on the initial relative phase of the two modes. If higher-frequency modes like this had actually been present in the initial conditions they would be affected by the generation of higher-frequency modes by the collapse of long wavelength perturbations. Obviously, there is no point in continuing the discussion to the interaction between three, four and n -modes.

But despite this complexity, what these examples show is that the relatively simple quantity D_k , defined by eq. (21), shows an interesting response to the non-linearity induced by mode coupling and which quantitatively encodes some of the structure seen in the return maps. In Section 5 we discuss how to exploit the information contained in this simple statistic in the analysis of more realistic distributions obtained from an arbitrary superposition of initial modes, rather than just two. We shall see that the clues obtained from the illustrative examples above suggest a new and potentially powerful method for the analysis of phase information.

4 PHASES FOR RANDOM PROCESSES

The previous section dealt with toy examples involving initial perturbations that were periodic on a given interval. In cosmology, the initial density field will not be periodic but will be in the form of one realisation of a random process. There are some subtleties involved in defining amplitudes and phases for such perturbations and these are often glossed over in the cosmological literature, although they are well known in the literature pertaining to random processes (e.g. Priestley 1981), so we will take the opportunity here to outline these problems and their resolution fairly carefully. In particular, a realisation of a random process can formally be expressed neither by a Fourier series (which assumes periodicity) nor a Fourier integral (which requires the function to tend to zero at $\pm\infty$). This section is about the correct mathematical way of treating the spectral representation of such a function, following the ideas of Wiener (1930).

To keep things as simple as possible and consistent with the previous section, consider a process $\delta(x)$ which is one realisation of a stochastic process on an infinite domain (i.e. one for which x can take any value on the real line). The generalisation of this to a three-dimensional field is entirely straightforward but the notation is more messy. Now consider the part of this realisation that lies in the range $-L \leq x < +L$. We can make a new function of $\delta(x)$ that is periodic by defining a new function $\delta_L(x)$ such that

$$\begin{aligned} \delta_L(x) &= \delta(x) \quad (-L \leq x \leq +L) \\ \delta_L(x + 2mL) &= \delta_L(x) \quad (m = \pm 1, \pm 2, \pm 3, \dots) \end{aligned} \quad (22)$$

The function δ_L is periodic with period $2L$ so let us express it as a Fourier series:

$$\delta_L(x) = \sum_{n=-\infty}^{+\infty} A_n \exp(ik_n x), \quad (23)$$

where $k_n = n\pi/L$ and A_n is given by

$$A_n = \frac{1}{2L} \int_{-L}^{+L} \delta_L(x) \exp(-ik_n x). \quad (24)$$

Thus,

$$\delta(x) = \frac{1}{\sqrt{2\pi}} \sum_{n=-\infty}^{+\infty} G_L(k_n) \exp(ik_n x) \Delta k_n \quad (25)$$

where $G_L(k)$ is defined, for any k , via

$$G_L(k) = \frac{1}{\sqrt{2\pi}} \int_{-L}^{+L} \delta_L(x) \exp(-ikx) dx = \frac{1}{\sqrt{2\pi}} \int_{-L}^{+L} \delta(x) \exp(-ikx) dx \quad (26)$$

where $\Delta k_n = k_{n+1} - k_n = \pi/L$. A spectral density function $P(k)$ can be defined by

$$P(k) = \lim_{L \rightarrow \infty} \langle \frac{|G_L(k)|^2}{2L} \rangle \quad (27)$$

where the expectation value $\langle \cdot \rangle$ is over the probability distribution. Note that $|G_L(k_n)| \rightarrow \infty$ as $L \rightarrow \infty$ but $|G_L(k_n)|\Delta(k_n) \rightarrow 0$ as $L \rightarrow \infty$.

Now we define the function $\tilde{\delta}_L(k)$ via

$$\tilde{\delta}_L(k) = \frac{1}{\sqrt{2\pi}} \int_{-\infty}^k G_L(q) dq, \quad (28)$$

so that

$$\Delta \tilde{\delta}_L(k_n) \equiv \tilde{\delta}_L(k_{n+1}) - \tilde{\delta}_L(k_n) \sim \frac{1}{\sqrt{2\pi}} G_L(k_n) \Delta k_n \quad (29)$$

for small values of Δk_n , i.e. for large L . Hence, in this limit,

$$\langle |\Delta \tilde{\delta}_L(k_n)|^2 \rangle \sim \langle |G_L(k_n)|^2 \frac{\Delta k_n}{2\pi} \rangle \Delta k_n = \langle \frac{|G_L(k_n)|^2}{2L} \rangle \Delta k_n \quad (30)$$

and, as $L \rightarrow \infty$ so that $\Delta k_n \rightarrow 0$

$$\langle |\Delta \tilde{\delta}_L(k_n)|^2 \rangle \sim P(k_n) \Delta k_n \sim \Delta Q(k_n), \quad (31)$$

where

$$Q(k) = \int_{-\infty}^k P(q) dq \quad (32)$$

is the integrated spectrum of $\delta(x)$.

The equation (25) provides a *spectral* representation for $\delta_L(x)$ for all x but which is only valid for $\delta(x)$ in the range $-L \leq x \leq +L$. To get a representation that is valid for all x we would like to let $L \rightarrow \infty$ in (25), but $G_L(k_n)$ does not converge to a finite value as $L \rightarrow \infty$. However, $G_L(k_n)\Delta k_n$ is well-behaved so we can write, in the range $-L \leq x \leq +L$,

$$\delta(x) \equiv \delta_L(x) = \sum_{n=-\infty}^{\infty} \Delta \tilde{\delta}_L(k_n) \exp(ik_n x). \quad (33)$$

Now is the time to let $L \rightarrow \infty$ so that $\Delta k_n \rightarrow 0$. The sum on the right-hand-side then converges in the required “mean-square” sense to a Stieltjes integral:

$$\delta(x) = \int_{-\infty}^{\infty} d\tilde{\delta}(k) \exp(ikx), \quad (34)$$

where

$$d\tilde{\delta}(k) = \lim_{L \rightarrow \infty} \Delta \tilde{\delta}_L(k_n). \quad (35)$$

The limit of equation (31) then becomes

$$\langle |d\tilde{\delta}(k)|^2 \rangle = dQ(k) = P(k) dk. \quad (36)$$

But note that $d\tilde{\delta}(k)$ is *not* the Fourier transform of $\delta(x)$; that role is more properly played by a term of the form $d\tilde{\delta}(k)/dk$. Following these considerations we can write

$$\tilde{\delta}(k_1) - \tilde{\delta}(k_2) = \frac{1}{2\pi} \int_{-\infty}^{+\infty} \left(\frac{e^{-ik_2 x} - e^{-ik_1 x}}{-ix} \right) \delta(x) dx. \quad (37)$$

The expression (37) has important consequences for the phases of the Fourier components of the process $\delta(x)$. First, note that $\langle \delta(x) \rangle = 0$. This requires that $\langle G_L(k) \rangle = 0$ which, in turn, means that $\langle \Delta\tilde{\delta}_L(k) \rangle = 0$ and this, in turn, means that $\langle d\tilde{\delta}_L(k) \rangle = 0$ for all k . Now, taking the complex conjugate of equation (34) yields

$$\delta^*(x) = \int_{-\infty}^{\infty} d\tilde{\delta}^*(k) \exp(-ikx) \quad (38)$$

and replacing x by $x + r$ in equation (34) yields

$$\delta(x + r) = \int_{-\infty}^{\infty} d\tilde{\delta}(k) \exp(ik(x + r)). \quad (39)$$

Multiplying these two expressions together and taking the expectation value leads to

$$\langle \delta^*(x) \delta(x + r) \rangle = \int_{-\infty}^{\infty} \int_{-\infty}^{\infty} \exp(ix[k' - k]) \exp(ik'r) \langle d\tilde{\delta}^*(k) d\tilde{\delta}(k') \rangle. \quad (40)$$

Since $\delta(x)$ is assumed to be statistically homogeneous, i.e. its probability distribution and all moments are invariant with respect to translations in x , the left-hand-side of this equation has to be the autocovariance function of the process $\xi(r)$. The right-hand-side must therefore be a function of r only. The contribution to the double integral must therefore vanish when $k \neq k'$. In other words,

$$\langle d\tilde{\delta}^*(k) d\tilde{\delta}(k') \rangle = 0 \quad (41)$$

if $k \neq k'$. This tells us immediately that the phases of the increments of the process, $\arg(d\tilde{\delta}(k)) = \phi_k$ must be random, in the sense that

$$\langle \exp i(\phi_k - \phi_{k'}) \rangle = 0 \quad (42)$$

for $k \neq k'$, since the above argument applies regardless of the form of $d\tilde{\delta}^*(k)$. The term *correlation* is usually taken to refer to the association expressed by expectation values like that on the left-hand-side of equation (42), i.e. second-order association. Statistical homogeneity thus requires that phases of the components of $\delta(x)$ should be *uncorrelated* and is not something to do with whether the process $\delta(x)$ is Gaussian. Notice also that the expectation value in equation (42) is an ensemble average, and this constraint does not apply necessarily to an average over a finite piece of a single realisation.

Of course the condition (42) does not mean that all phases must be statistically independent; it is weaker than the requirement that the joint probability distributions of two phases be separable. Neither does it mean that no statistical quantity based on the ϕ_k recovered from a single realisation can be found that is sensitive to the non-Gaussianity of $\delta(x)$. What it does show, however, is that one has to look further than methods based on second-order properties of the distribution of phases. This is the challenge we address in the next section.

5 QUANTIFYING PHASE INFORMATION

5.1 Preamble

From the examples discussed in Section 3, one can see that the signature of non-linear mode coupling is that the phases of the Fourier modes on large scales couple in certain relationship, depending on the morphology of the density distribution. On smaller scales, however, the phases queue up in such a way that phase difference, or the discrete phase gradient D_k , converges. This suggests that it might be a good idea to construct a histogram of the phase gradients for each mode and use it as a test of phase correlations, interpreted in the wider sense. In a Gaussian random field, the phases are random, so the phase gradient will simply be the difference between two uniformly-distributed random variables and will itself be uniformly distributed between $-\pi$ and π . For a non-Gaussian field, however, this might not be the case. The distribution of phase differences is therefore one possible way of using phase information as a diagnostic of non-Gaussianity. Notice that this histogram is more useful than the histogram of phases themselves, which would simply be the projection of a return map onto one of its axes: this would be uniform even in the highly structured distributions seen in the previous section. Although this particular approach is suggested by the convergence displayed in the simple examples shown above, there could of course be other forms of phase behaviour that it might also quantify.

Taking a histogram from a set of data produces something more-or-less equivalent to a probability density distribution. We can exploit this idea to think of the information content of this probability density, by defining a quantity analogous to its entropy. At the start, however, we should stress that this should by no means be interpreted as a thermodynamic entropy, as it only relates to the pattern of phases and not to the whole spatial distribution of material in space.

5.2 Phase entropy

We now define a quantity, the *phase entropy*, as

$$S = - \sum_{-\pi}^{\pi} \rho_i(D_k) \ln [\rho_i(D_k)] \delta\phi_i, \quad (43)$$

with

$$\sum \rho_i \delta\phi_i = 1, \quad (44)$$

where $\rho_i(D_k) \delta\phi_i$ is the probability of finding a value in the i -th bin. This definition takes into account changes in binning strategy for the construction of the histograms. If $\delta\phi_i$ were infinitesimal,

$$S = - \int_{-\pi}^{\pi} \rho(D_k) \ln [\rho(D_k)] d\phi. \quad (45)$$

If a data set consisting of n_{tot} values of D_k is binned into a histogram of m bins, each of which has width $\delta\phi = 2\pi/m$, the probability density for n events in the i -th bin is $\rho_i = n/(n_{\text{tot}} \delta\phi_i)$.

Now another virtue of D_k becomes apparent. The phase of each Fourier mode changes with the choice of origin, and so does the converging point of phase gradient. Any statistic we use should not depend on the choice of origin, or at least this should be easy to remove from the calculations. Changing the point of origin by a distance x changes the phase of the k -th mode by an amount kx , so the effect on the individual phases depends on their wavenumber. But the phase gradient suffers a constant offset

$$D_k = \phi_{k+1} + (k+1)x - \phi_k + kx = \phi_{k+1} - \phi_k + x = D_k + x, \quad (46)$$

which can be handled easily. Now take as an example a single density peak, located at a . The phase for the k -th mode is $-ka$, so the phase gradient for all k values of the Fourier decomposition of the density peak converges to the same value,

$$D_k = \phi_{k+1} - \phi_k = -(k+1)a - (-ka) = -a. \quad (47)$$

The probability density distribution is the same for all values of a , even with a constant offset caused by different choice of origin. This approach to phase information weights all phases equally, and discards power spectral information. As shown in the previous sections, the way in which the Fourier phases queue up depends on the relative level of the most dominant density peak to the rest of the structure: the higher the dominant peak, the greater is the effect for large k . It is the 'queuing up' of phases of high-frequency modes that signifies the gravitational clustering towards the nonlinear regime, quite independently of the amplitude corresponding to each phase. The quantity D_k encodes information about the ratio of successive Fourier components:

$$\frac{\tilde{\delta}_{k+1}}{\tilde{\delta}_k} = \frac{|\tilde{\delta}_{k+1}|}{|\tilde{\delta}_k|} \exp[i(\phi_{k+1} - \phi_k)] = A \exp(iD_k), \quad (48)$$

where A is a real number, which is obviously neglected in our analysis. This is a potential weakness when it comes to applying these ideas in practice, because a mode with vanishing amplitude still has a phase which receives equal weight in D_k with those of much higher amplitude. In real applications, therefore one would probably want to combine amplitude and phase information in some way, perhaps by removing modes of very low amplitude from the analysis. We return to this in Section 7. For the rest of this paper we shall neglect this problem and look at phase-only information.

The idea of phase entropy was suggested by Polygiannakis & Moussas (1995). It comes directly from Boltzmann's definition of entropy in thermodynamics. In an ensemble of ν identical replicas, the statistical weight Ω_ν of its system when ν_1 are in state 1, ν_2 in state 2, ..., and ν_r in state r is

$$\Omega_\nu = \frac{\nu!}{\nu_1! \nu_2! \cdots \nu_r!}. \quad (49)$$

The entropy of the ensemble is thus $S_\nu \sim \ln \Omega_\nu$. If ν is sufficiently large, ν_r also become large, so $\ln \Omega_\nu \sim \nu \ln \nu - \sum_r \nu_r \ln \nu_r$. Taking $p_r = \nu_r/\nu$, the probability of state r , we reach $S \sim - \sum_r p_r \ln p_r$. In the analogy to the definition of phase entropy, r microstates correspond to the bins in a histogram, which are between $-\pi$ and π . Following the work of Shannon (1948a,b) this definition of entropy S is closely related to the information content I of the distribution: $S(D) = -I(D)$. We do not wish to push the connection with Boltzmann entropy too far, however, and in any case the definition of phase entropy is self-contained. It is not necessary to think about an approximation scheme of Ω_ν , i.e., requiring ν to be very large. Nevertheless, it is still required to have large enough of phases so as to produce a smooth probability density distribution. In some cases, where the probability density distributions are highly skew

and therefore some bins in the histogram might have zero number density, the contribution to phase entropy from these bins is zero, as $\lim_{\rho_r \rightarrow 0} \rho_r \ln \rho_r = 0$.

For a Gaussian field, where the number of Fourier modes is sufficiently large, and the phases of each of these modes are random, the phase entropy is

$$S = - \sum \rho_i \ln \rho_i \delta\phi_i = - \int_{-\pi}^{\pi} \rho(D_k) \ln [\rho(D_k)] d\phi = - \int_{-\pi}^{\pi} \frac{1}{2\pi} \ln \left(\frac{1}{2\pi} \right) d\phi = \ln 2\pi. \quad (50)$$

It can be proven, by straightforward analogy with the isoperimetric problem of variational calculus, that phase entropy has its maximal value when the probability density function $\rho[D_k] = 1/2\pi$ is constant. The Gaussian process, wherein the distribution of phases (and phase differences) is uniform, corresponds to a state of maximum entropy, and the value of $S = \ln 2\pi$ is the maximum value that S can take in any situation.

When an initially-Gaussian field evolves under gravitational instability, the phases 'queue up' in a certain fashion, and the phase gradient is no longer evenly distributed in the histogram. What happens then is that the entropy of the phases *decreases* or, in other words, the information content increases. This does not mean that the process violates the second law of thermodynamics, because information moves between the amplitudes and phases (and indeed, between the density and velocity parts of phase-space) as the system evolves. There is more information in the whole system than is contained only in the phases, but the information content of these phases does certainly increase under the action of gravitational clustering.

Although our application of this idea is largely inspired by Polygiannakis & Moussas (1995), who applied it to the analysis of time-varying quantities in Solar Wind data, they did not take into account the fact that the straightforward $p \log p$ entropy of the phase histogram itself is not invariant under translations of the origin. In our application, we use $S(D)$ rather than $S(\phi)$ to counter this problem, as above.

6 NUMERICAL SIMULATIONS

In order to study the behaviour of S in systems with more complex initial data, we have conducted a series of numerical N-body experiments. In order to keep these experiments as simple as possible and to obtain the best possible numerical resolution with the computer resources available to us, we have used two-dimensional simulations of 512^2 particles on a 512^2 mesh (like those described in Beacom et al. 1991).

Four different initial pure power law spectra $P(k) \propto k^n$ are modelled (with $n = 2, 1, 0$, and -1) for each of which the initial phases are randomised using a random number generator. To see the systematic effects from different power spectral indices and exclude the influence from phases, we set the same phases for the same modes for each of the 4 spectral indices. The boundary of each realisation is periodic. The simulations are equivalent to 3D Einstein-De Sitter ($\Omega = 1$) universe with 2D perturbations, whose images are cross sections of 3D perturbations. The spectral index n in 2D is equivalent to $n - 1$ in 3D in statistical measure. We also label the evolutionary stages of the simulations according to k_{NL} where

$$\langle (\delta\rho/\rho)^2 \rangle_{k_{NL}} = b_+^2(t) \int_0^{k_{NL}} P(k) d^2k = 1. \quad (51)$$

Here $b_+(t)$ is the growing mode in (7) of the linear density contrast, and $P(k)$ is the linear extrapolation of the initial power spectrum. This definition of k_{NL} identifies the corresponding $2\pi k_{NL}^{-1}$ as the boundary between linearity and non-linearity. From this criterion and $P(k) \propto k^n$, $k_{NL}^{n+2} \propto b_+^{-2}(t) \propto (1+z)^2$. We set the final stage of the simulations the final stage to have $k_{NL} = 2$, and pick 8 stages with values of k_{NL} varying by a factor of two in each one; the first stage has $k_{NL} = k_{\text{Nyquist}} = 256$.

Before proceeding, it is worth illustrating the points we made in the introduction about the importance of phase information using these simulations.

To extract a measure of the phase entropy from these two-dimensional N-body simulations, we simply take the probability density distribution of all phase gradients in k_x direction, for S_x , and those in k_y direction, for S_y , then we take the arithmetic mean, because of the additive nature of the definition. To express in a clearer way, we can, for example, write

$$S_x = - \sum_{i=1}^m \rho(D_{k_x}) \ln [\rho(D_{k_x})] \delta\phi_x, \quad (52)$$

where

$$D_{k_x} = \phi(i+1, j) - \phi(i, j) \quad (53)$$

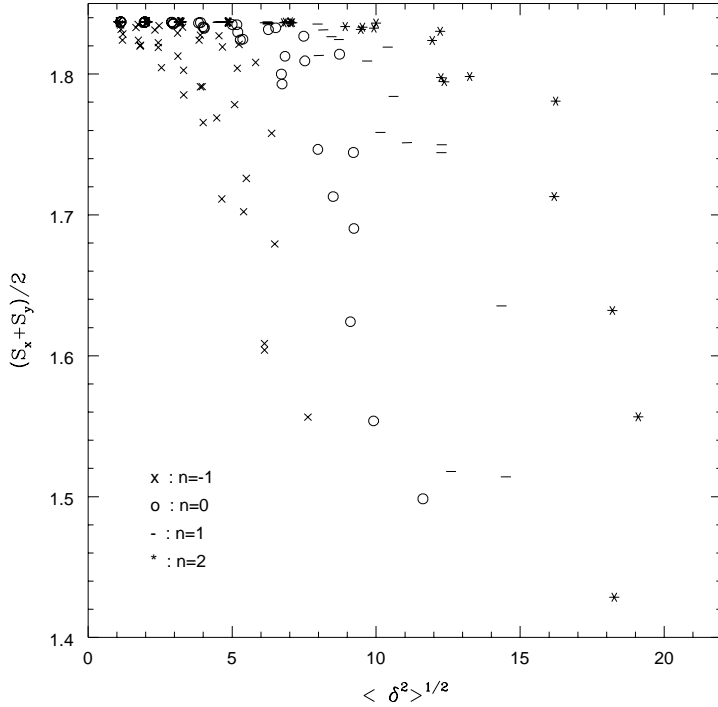


Figure 5. Phase entropy of the gravitational evolution from different initial power spectral indices is shown as a function of the *rms* density fluctuations. For each spectral index, N-body simulation for 5 initial conditions of different random phases are conducted. Phase entropy, at its maximal value $\ln 2\pi$ at the start, decreases when the system evolves. The different spectral indices display different characteristic curves of this decrease in phase entropy.

for $1 \leq i, j \leq 256$, the upper limit being the Nyquist frequency of the simulations. The number of bins m is chosen according to the number of phases available, to ensure the probability density distribution is reasonably smooth. For a realisation of 512^2 particles on a 512^2 mesh, there are 256^2 phases. The phase gradient $D(k_x)$ for a certain j is the phase gradient for the corresponding strip in the x -direction of the density distribution in real space. By taking all the phase gradients in one direction, binning them into a histogram, we are scanning every strip and examining the morphology of the realisation in that direction.

Phases not only suffer an offset at the choice of origin in real space, but also depend upon orientation. In reality there should not be any preferred orientation in which the phase entropy is calculated. If a large filament lies diagonally across a realisation, it intercepts with every strip of the realisation at different positions. The converging points of the phase gradient for every strip cover the interval $[-\pi, +\pi]$ uniformly, and each contributes the same amount of number density to every bin in the histogram. This results in a large phase entropy. However, if we rotate the realisation so that the strip lies across the scanning direction, a lower value of S will be obtained. Here in Figure 5 all of the realisations are rotated to the orientation along which the phase entropy is at its minimal value.

We perform 5 sets of different initial phases, so there are 40 realisations for each spectral index. In Figure 5, we plot the phase entropy against the variance of the density field in the realisation for all power spectra. (The variance is plotted by smoothing the density field onto the the grid using a box-counting algorithm).

It is immediately clear that the phase entropy decreases as the density variance increases, in other words as the system evolves. This is in full accord with our intuition described above, and confirms that S is a potentially useful diagnostic statistic. Furthermore, the different spectral indices display different characteristic curves of this decrease in phase entropy. The trends can be explained qualitatively in terms of the known morphology of clustering generated by the different sets of initial conditions. The spectrum with $n = -1$ contains a relatively large amount of power in long-wavelength modes. The evolution of a system with this initial spectrum is characterized by the early generation of long filaments where the caustics form; sheets form in 3D, but these are not relevant to the 2D simulations used here. In this case we can always rotate the realisation so that the longest filament, which has the largest effect on S is parallel (or perpendicular) to the orientation along which the Fourier transform is performed. The phase entropy decreases on the formation of large filaments of size similar to the simulation box, which happens even when the variance is small. As n decreases so does the amount of large-scale power. In order to produce the large filaments

that result in a decrease of S , the system has to evolve further on small scales. In the most extreme case of $n = 2$, this results in a very high value for the variance when S starts to display phase structure.

6.1 Scaling and Self-similarity

Before further application of phase entropy, we have to address some important features of the simulations from initial pure power law spectra. The initial pure power law spectra possess no characteristic length scales and also evolves in a self-similar manner, which means that at different stages, the distribution should possess the same. For a self-similar physical system, time dependence can be singled out by rescaling \mathbf{x} , the spatial position, or \mathbf{p} , the momentum. Therefore a distribution function $f(\mathbf{x}, \mathbf{p}, t)$ has the same statistical measure as the rescaled one, $\lambda^\alpha f(\mathbf{x}/\lambda^\beta, \mathbf{p}/\lambda^\nu, \lambda t)$, as $t \rightarrow \lambda t$, where α , β , and ν are to be decided (Jain & Bertschinger 1996). Self-similar gravitational clustering is an idealisation and can not be applied in detail to a realistic model. It nevertheless provides useful insights into more realistic situations.

Since the phases of Fourier modes play an important role in recovering the morphology of a density distribution (Oppenheim & Lim 1981), it is interesting to see if there is any self-similar scaling of the phases in gravitational evolution. As well as the 512^2 N-body simulations discussed in the previous section, we also conduct 2048^2 simulations with initial pure power law spectra, $n = 2, 1$, and 0 . With $k_{NL} = 2$ as the final stage ($z = 0$), there are 10 stages, denoted stage $a, b \dots j$. To distinguish large- and small-scale phases, a realisation of a 2048^2 simulation box is divided into 2^2 (scale length $l_s = 2048/2 = 1024$), 4^2 ($l_s = 512$), 8^2 ($l_s = 256$), 16^2 ($l_s = 128$), etc. boxes (sub-realisations). On each scale length l_s , we calculate the phase entropy for each sub-realisation, and then take average of them over that scale. By doing so, we are averaging phase entropy for the same scale length through many sub-realisations. The lower limit of the scale length of sub-realisations chosen is the one which still has sufficient large number of phases. Here we choose as the smallest scale length $l_s = 64$, by dividing a 2048^2 realisation into 1024 sub-realisations of a 64^2 mesh. Each 64^2 mesh offers merely 32^2 phases binned into a histogram of 40 bins. Therefore, for each 2048^2 realisation, the phase entropy appears on 5 different scale lengths, and, from large to small l_s , more and more phases from large scales are excluded from the calculation. It is expected that phase entropy decreases through large to small scales, as structure on small scales goes nonlinear while that on large scales is still in the linear regime. To simplify the calculations and for completeness, the sub-realisations are not rotated to minimise the phase entropy in this case. Taking $l_s = 512$ as an example, we divide a realisation of a 2048^2 simulation box into $(2048/512)^2 = 16$ sub-realisations, each of which is a 512^2 mesh, and calculate the phase entropy for each sub-realisation, before taking average of the phase entropy of these 16 sub-realisations. Structure scales larger than 512 , $1/4$ of the side of the whole simulation box, are left out, what is included in the calculation being the structure up to the scale length l_s .

In Figure 6, the phase entropy is shown on 5 scale lengths for stage f to j . The phase entropy decreases from large to small l_s for all three spectral indices. For stage g of spectral index $n = 2$, the phase entropy decreases drastically from scale length $l_s = 128$, to $l_s = 64$, which can be viewed as follows. The stages of simulations are chosen to indicate the boundary between linearity and nonlinearity and that there is factor of two between any two adjacent stages. For stage g ($k_{NL} = 16$), the boundary is on a box size of $(2048/16)^2 = 128^2$, meaning that structure within a 128^2 box placed anywhere in the simulation box has gone nonlinear in a statistical sense. Thus the transition from linearity to nonlinearity across the boundary is shown clearly via the large decrease of the phase entropy from length scale $l_s = 128$ to $l_s = 64$. The same situation applies to stage h from $l_s = 256$ to $l_s = 128$, where $l_s = 256$ corresponds to the boundary size of nonlinearity; so does stage i from $l_s = 512$ to 256 , and stage j from $l_s = 1024$ to 512 . What is more interesting in Figure 6 is that phase entropy seems to stay at the same level for the same degree of nonlinearity in the plot. Stage g at scale length $l_s = 64$ possesses the same level of phase entropy as stage h at $l_s = 128$, so does stage i at $l_s = 256$, and stage j at $l_s = 512$. If k_{NL} is used to denote the stages, $S(k_{NL}, l_s) = S(2, 512) \sim S(4, 256) \sim S(8, 128) \sim S(16, 64)$. This result is not surprising at all. As k_{NL} are chosen twofold for two adjacent stages in the self-similar evolution, the distribution of stage m looks the same statistically as stage $m+1$ when blown up by a factor of two. For any scale length l_s of stage m , it should retain the same level of phase entropy as the next stage $m+1$ at double scale length, $2l_s$. Therefore, the phase entropy is indeed an indicator of the level of nonlinearity (or linearity), and demonstrates the roughly self-similar nature of the evolution, which can be expressed as

$$S(k_{NL}, l_s) = S(2k_{NL}, l_s/2), \quad (54)$$

as $k_{NL} \rightarrow 2k_{NL}$, or equivalently, $(1+z) \rightarrow 2^{\frac{n+2}{2}}(1+z)$. All the stages can be scaled by phase entropy into one single characteristic curve, $S(k_{NL}l_s)$.

This simple picture is complicated by a number of factors which produce a discernible slope in Figure 6, which displays a perceptible tilt toward small l_s . This disagreement between points of the same level of nonlinearity may be due to the fact that S does not scale in a self-similar fashion. But before this can be concluded we have to

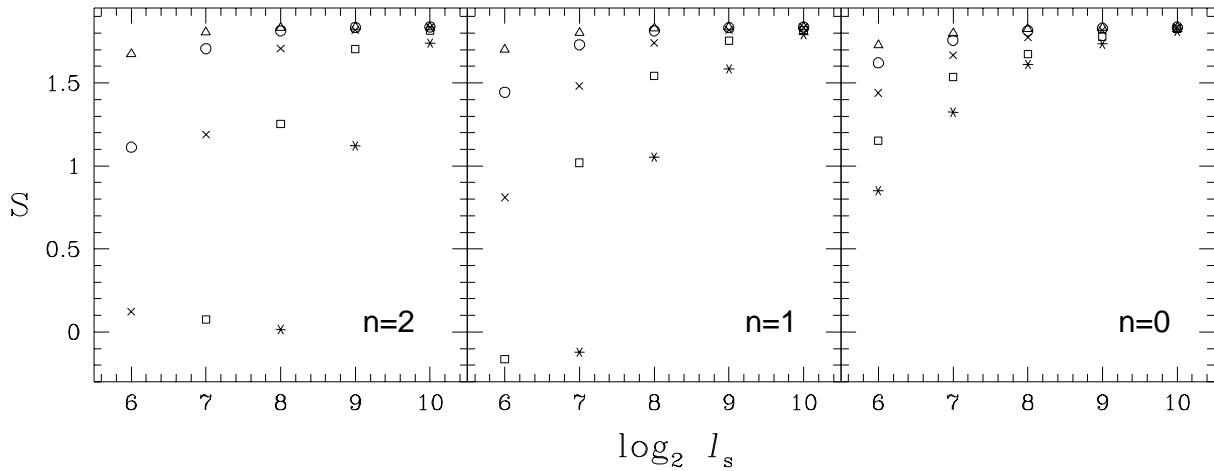


Figure 6. The phase entropy is shown for five length scales $l_s = 64, 128, 256, 512$ and 1024 . \triangle denotes stage f , \circ denotes stage g , \times stage h , \square stage i , and $*$ stage j . Clearly, phase entropy decreases towards small length-scale as expected. For the same stage of $n > 0$, the transition in scale from linearity to nonlinearity can be seen from the large decrease in phase entropy by decreasing l_s , e.g., for stage g from $l_s = 128$ to 64 , stage h from $l_s = 256$ to 128 , stage i from $l_s = 512$ to 256 , and stage j from $l_s = 1024$ to 512 . Also phase entropy seems an indicator to nonlinearity of gravitational clustering. The amount of decrease in phase entropy is roughly the same for the transition from linearity to nonlinearity for every stage, which implies self-similar nature of gravitational clustering for pure power law spectra.

contend with several complicating factors. First, for large l_s , there are fewer sub-realisations to be averaged, and the sub-realisations in this experiment are not rotated to obtain the value of the phase entropy. This is expected to artificially increase the phase entropy on large-scales compared to small. This is probably more pronounced for small n where filaments dominate. For small l_s the averaging of more sub-realisations erases this effect. Using larger bins to compensate for the smaller number of phases available also lowers the phase entropy. We therefore see points at the same level of phase entropy tilt towards small length scales. Another numerical effect comes in when both k_{NL} and l_s are small. In forming clusters, galaxies aggregate at the expense of forming voids. When the evolution goes into the highly nonlinear regime, voids dominate the realisation and many of the sub-realisations become empty. This produces an artificial contribution to the entropy determined partially by the bin size.

But while the exact form of scaling remains to be determined by eliminating these possible systematics and studying the scaling of S for a wider range of spectral indices, this study at least shows that phase entropy has qualitatively the right properties for a diagnostic of gravitational evolution.

7 DISCUSSION AND CONCLUSIONS

The aim of this paper was to explore the behaviour of phases of Fourier components of cosmological density fluctuations in order to understand how phase information relates to the development of clustering pattern from random-phase (Gaussian) initial conditions.

We have studied some simple cases of the evolution of Fourier phases under the action of gravitational instability and used these cases to motivate the definition of a measure of the information contained in these phases. The statistic we propose, S , which behaves as a kind of information entropy, shows interesting time-evolution and appears to undergo a form of scaling when the initial conditions on which gravity acts are self-similar.

Although this statistic looks like a promising candidate as a diagnostic for phase coupling, there are many problems to be overcome before it can be applied to real data. For example, it remains to be seen how S can be corrected for shot-noise (discreteness) errors and also how to correct for the imposition of a selection function. Redshift-space effects also need to be taken into account. These are inevitably more difficult to handle for a higher-order statistic than with the correlation function or the power-spectrum. There is also the problem, alluded to in Section 5, that even Fourier modes with negligible amplitudes have a phase, and our statistic does not take account at all of amplitude information. In a practical application one would probably therefore prefer to combine amplitude information with phase information. This is what is done to some extent with the bispectrum (Matarrese et al. 1997) and the second spectrum (Stirling & Peacock 1996). But note that the bispectrum, for example, only contains

information about third-order moments of the Fourier components. It does not therefore include all the information that resides in the distribution of phases. Knowledge of all higher-order polyspectra would be necessary to define the total information content of the Fourier phases. For this reason it is certainly worth investigating statistics based explicitly on the phases, rather than indirectly on them as is done with the bispectrum or any other piecemeal approach higher-order moments.

In future we hope to test the usefulness of phase statistics compared with more standard methods. In any case we stress the point that phase information is completely complementary to amplitude information: no information about localised geometrical structures is contained in the amplitudes themselves, so phase information however it is encoded is vital to a full analysis of clustering pattern.

As we discussed in the introduction, phase information *per se* has not been extensively used in galaxy clustering analyses so far. We hope to develop tools that use this information to provide sensitive tests of cosmological models. In the context of galaxy clustering, what we need to understand using further N-body experiments is how the growth of phase information relates to the growth of the power spectrum. It is known that gravitational instability acts on initially Gaussian perturbations to produce fluctuations that are non-Gaussian but which are characterised by higher-order moments, such as the skewness $\langle \delta^3 \rangle$ that couple to the variance $\langle \delta^2 \rangle$ in a well-defined way (e.g. Coles & Frenk 1991; Bernardeau 1992). One of the possibilities we shall explore is how the growth of phase information itself couples to the growth of the Fourier amplitudes. If this coupling can be quantified, then one can hope to use it as a diagnostic of clustering. For example, many clustering models appeal to the presence of a bias to enhance the clustering pattern over that generated by gravity (e.g. Coles 1993). A linear bias b affects the Fourier amplitudes but not their phases. One can therefore hope to distinguish a biased power spectrum from one generated solely by gravitational instability: for the same amplitude, the former should have a higher phase entropy (lower phase information) than the latter. By quantifying the phase information on very large scales we also hope to test initial non-Gaussianity, if the non-Gaussianity developed from initially Gaussian fluctuations can be understood. We shall return to these and related questions in future work, but the scaling described in Section 6 is grounds for optimism that this can be achieved.

We also take this opportunity to point out that the phase entropy can in principle be applied not just to density fluctuations, but also as a diagnostic of non-Gaussianity in microwave background temperature fluctuations. With tentative claims already being made for the detection of non-Gaussian effects in the COBE data in an analysis based on bispectra (Ferreira, Magueijo & Gorski 1998), though not without opposition (Bromley & Tegmark 1999), the pre-Planck development of sensitive yet robust statistical indicators is a matter of urgent priority. Phases can be defined for a spherical harmonic expansion in a similar way to that of the Fourier modes and may provide more information about the form of non-Gaussian behaviour present in existing CMB maps as well as offering more powerful and sensitive descriptors of future data sets.

REFERENCES

Bardeen J.M., Bond J.R., Kaiser N., Szalay A.S., 1986, ApJ, 304, 15
 Beacom J.F., Dominik K.G., Melott A.L., Perkins S.P., Shandarin S.F., 1991, ApJ, 372, 351.
 Bernardeau F., 1992, ApJ, 391, 1.
 Bromley B.C., Tegmark M., 1999, preprint, astro-ph/9904254
 Coles P. Frenk C.S., 1991, 253, 727
 Ferreira P.G., Magueijo J., Gorski K.M., 1998, ApJ, 503, L1
 Jain B., Bertschinger E., 1996, ApJ, 456, 43
 Jain B., Bertschinger E., 1998, ApJ, 509, 517
 Matarrese S., Verde L., Heavens A.F., 1997, MNRAS, 290, 651
 May R.M., 1976, Nature, 261, 459
 Oppenheim A.V., Lim J.S., 1981, Proc. I.E.E.E., 69, 529
 Peebles P.J.E., 1980, The Large-scale structure of the Universe. Princeton University Press, Princeton.
 Polygiannakis J. M., Moussas X., 1995, Solar Physics, 158, 159
 Priestley M.B., 1981, Spectral Analysis and Time Series. Academic Press, London.
 Ryden B.S., Gramann M., 1991, ApJL, 383, L33
 Sahni V., Coles P., 1995, Physics Reports, 262, 1
 Scherrer R.J., Melott A. L., Shandarin S. F., 1991, ApJ, 377, 29
 Shandarin S.F., Zel'dovich Ya. B., 1989, Rev. Mod. Phys., 61, 185
 Shannon C., 1948, Bell System. Tech. J., 27, 379.
 Soda J., Suto Y., 1992, ApJ, 396, 379
 Stirling A.J., Peacock J.A., 1996, MNRAS, 283, L99
 Wiener N., 1930, Acta Math., 55, 117
 Zel'dovich Ya.B., 1970, A&A, 5, 84

This figure "fig1.gif" is available in "gif" format from:

<http://arxiv.org/ps/astro-ph/9905250v2>